Planta (2006) 224:1279–1290
DOI 10.1007/s00425-006-0307-z

ORIGINAL ARTICLE

# Nuclear fragmentation and DNA degradation during programmed cell death in petals of morning glory (*Ipomoea nil*)

**Tetsuya Yamada · Yasumasa Takatsu · Masakazu Kasumi · Kazuo Ichimura · Wouter G. van Doorn**

Received: 24 February 2006 / Accepted: 25 April 2006 / Published online: 1 June 2006


**Abstract** We studied DNA degradation and nuclear fragmentation during programmed cell death (PCD) in petals of *Ipomoea nil* (L.) Roth flowers. The DNA degradation, as observed on agarose gels, showed a large increase. Using DAPI, which stains DNA, and flow cytometry for DAPI fluorescence, we found that the number of DNA masses per petal at least doubled. This indicated chromatin fragmentation, either inside or outside the nucleus. Staining with the cationic lipophilic fluoroprobe $DiOC_6$ indicated that each DNA mass had an external membrane. Fluorescence microscopy of the nuclei and DNA masses revealed an initial decrease in diameter together with chromatin condensation. The diameters of these condensed nuclei were about 70% of original. Two populations of nuclear diameter, one with an average diameter about half of the other, were observed at initial stages of nuclear fragmentation. The diameter of the DNA masses then gradually decreased further. The smallest observed DNA masses had a diameter less than 10% of that of the original nucleus. Cycloheximide treatment arrested the cytometrically determined changes in DNA fluorescence, indicating protein synthesis requirement. Ethylene inhibitors (AVG and 1-MCP) had no effect on the cytometrically determined DNA changes, suggesting that these processes are not controlled by endogenous ethylene.

**Keywords** DNA degradation · DNA mass · Nuclear fragmentation · Petal senescence · Programmed cell death · Wilting

**Abbreviations**

| | |
|---|---|
| AVG | Aminoethoxyvinyl glycine |
| CHI | Cycloheximide |
| DAPI | 4,6-Diamidino-2-phenylindole |
| $DiOC_6$ | 3,3′-Dihexyloxacarbocyanine iodide |
| 1-MCP | 1-Methylcyclopropene |
| PCD | Programmed cell death |

## Introduction

Programmed cell death (PCD) during normal plant development is characterised by organised degradation of most organelles, followed by rupture of the tonoplast. After tonoplast rupture, the released enzymes result in rapid degradation of what remains of the cell (Obara et al. 2001). Changes in the nucleus during plant PCD usually include chromatin condensation and degradation of proteins and nucleic acids. In some cells, this is accompanied by fragmentation of the chro-

T. Yamada · Y. Takatsu · M. Kasumi
Plant Biotechnology Institute,
Ibaraki Agricultural Center,
319-0292 Ibaraki, Japan

T. Yamada · K. Ichimura
National Institute of Floricultural Science,
305-8519 Ibaraki, Japan

W. G. van Doorn
Wageningen University and Research Centre,
P.O. Box 17, 6700 AA Wageningen,
The Netherlands

*Present address*: T. Yamada (✉)
Graduate School of Agriculture,
Tokyo University of Agriculture and Technology,
183-8509 Tokyo, Japan
e-mail: teyamada@cc.tuat.ac.jp

matin into a number of smaller masses, which may represent nuclear fragmentation (Wang et al. 1996; Danon and Gallois 1998; Yao et al. 2004). In other plant cells no apparent fragmentation of the chromatin occurs during PCD; hence no nuclear fragmentation takes place. Only following vacuolar rupture the nucleus rapidly disappears (Obara et al. 2001).

Relatively little is known about the details of nuclear fragmentation during plant cell PCD. This is in contrast with animal PCD. Transmission electron microscopy of apoptotic cells showed that the nucleus often becomes fragmented whereby each part remains surrounded by a membrane, and that the fragments are transferred to apoptotic bodies (Boe et al. 1991; Dini et al. 1996; Sun et al. 2000).

The PCD in animals is often categorised into three types: (1) apoptosis, which ends in degradation inside the lysosome (vacuole) of another cell, (2) autophagy, which is a mechanism whereby the cell degrades itself, mainly by lysosomal activity, and (3) non-lysosomal death, based mainly on a mechanism other than lysosomal action. Nuclear fragmentation is considered to be common in apoptotic cells (Hockenbery 1995), but may also occur in the other types of PCD. In plants, no true apoptosis seems to occur, whereas autophagic and non-lysosomal PCD are apparently common (van Doorn and Woltering 2005). It is not clear if these categories of plant PCD would in any way coincide with the presence or absence of nuclear fragmentation, and with the kind of fragmentation.

Nuclear fragmentation should be distinguished from chromatin fragmentation. If the chromatin fragments into some large masses inside the original nuclear membrane the process must be called chromatin fragmentation and not nuclear fragmentation. Several papers on the plant PCD show that the chromatin in a cell becomes fragmented into a number of DNA masses. This can mean one of the four things: (1) the chromatin becomes fragmented into large masses inside the same nuclear membrane, (2) the fragmentation resulted in DNA masses that are each surrounded by a membrane, (3) the chromatin has become fragmented into masses each without a surrounding membrane, and (4) a combination of (1)–(3). The phenomena 2 and 3 may be called nuclear fragmentation.

Wang et al. (1996) studied PCD in toxin-treated tomato protoplasts. Numerous bodies, close to the cell periphery, stained with Hoechst 33342, a probe for DNA. Although it was claimed that these bodies were the result of nuclear fragmentation, the authors did not check whether these DNA masses were inside the nuclear membrane or not. Danon and Gallois (1998) observed PCD in *Arabidopsis* protoplasts treated with UV radiation. Many round-shaped DNA masses were observed at the cell periphery. Again it was not shown if these masses were still inside a nuclear membrane. Yao et al. (2004) similarly showed that the chromatin in the cell became fragmented, but did not show if the DNA masses were inside the original nuclear membrane or not, and if not, if they each were surrounded by a membrane. Finally, in previous work from one of our labs we also showed fragmentation of the chromatin during plant PCD, using flow cytometry (Marubashi et al. 1999; Yamada et al. 2001, 2003). These data also did not allow a distinction between the earlier possibilities (1)–(4).

We now used the ephemeral *Ipomoea nil* flower as a model. *I. nil* and the closely related *I. tricolor* have been widely used in previous studies on petal senescence (Winkenbach 1970; Matile and Winkenbach 1971; Baumgartner et al. 1975; Beutelmann and Kende 1977). The purpose of the present paper was to establish if there is chromatin fragmentation or nuclear fragmentation during PCD in the petals of this species, and if so, how its time line is related to other PCD parameters. Our hypotheses were: (1) nuclear DNA degradation in *Ipomoea* petal cells occurs prior to cellular collapse, and (2) nuclear fragmentation occurs.

## Materials and methods

### Plant material

Seedlings of *I. nil* (L.) Roth cv. Violet (seeds from Marutane Co., Kyoto, Japan) were grown in a controlled chamber at 24±1°C, about 70% relative humidity (RH) and 13 h per day cool-white fluorescent light (100 μmol $m^{-2}$ $s^{-1}$). The light period was from 0800 to 2100 hours. The flowers were almost fully open when the lights turned on.

### Colour change and petal inrolling

The colour of the abaxial surface of the merged petals, between the midribs, about halfway from the distal edge and the petal base, was measured with a CR-400 colorimeter (Konica Minolta Co., Ltd., Tokyo, Japan). Colorimetric values were determined using the CIE $L^*a^*b^*$ system, and hue angles ($h°$) were calculated from the $a^*$ and $b^*$ values according to McGuire (1992). The average was obtained from values in three parts of each corolla.

For inrolling, the abaxial surface of the petals was photographed horizontally. The diameter aligned with

the midrib of the merged petals was measured by SimpleDigitizer version 3.01 software for image analysis (free to download at http://www.vector.co.jp/). The means was calculated from the diameters of five positions on each corolla. The inrolling index was calculated as the percentage decrease from the maximum diameter.

## DNA degradation

The DNA breakdown was detected by agarose gel analysis and by flow cytometry. For gel analysis, total DNA was extracted according to Yamada and Marubashi (2003). The DNA solution was immediately electrophoresed in a gel containing 3% agarose and stained with SYBR Gold nucleic acid gel stain (Molecular Probes, Eugene, OR, USA). The gel pattern was photographed, using an electronic UV transilluminator system (model FAS-III mini + DS-30; Toyobo, Tokyo, Japan). The DNA degradation pattern was also scanned using the STORM 830 PhosphorImager system (Amersham Biosciences), which quantitatively detects fluorescence intensity. The DNA degradation index was calculated using CS Analyzer Version 2.02b (Atto, Tokyo, Japan), software for DNA analysis. The DNA degradation index is the percentage of signal intensity between fragmented DNA (area B in Fig. 1c) and total DNA (area A in Fig. 1c). In Fig. 1c the DNA degradation index values under the gel pictures are means of three gels, one flower per gel.

The DNA levels were also estimated by flow cytometry (Yamada et al. 2003). Briefly, the petals were chopped in nuclear extraction buffer, which was included in the high resolution kit for Plant DNA (Partec, Münster, Germany), a reagent set provided by the manufacturer of the flow cytometer. The extraction buffer is a low pH solution containing Triton X-100. The extract was filtered through 50-μm nylon mesh. The medium with the isolated nuclei was collected, the buffer with the fluorescent DNA stain 4,6-diamidino-2-phenylindole (DAPI) from a standard reagent set (Partec) was added, and the solution was vortex mixed. The DNA content of the isolated nuclei was analysed using a flow cytometer (Ploidy Analyzer, Partec). The DNA levels were obtained in a total of 10,000 nuclei. It should be noted that the large histogram peak was adjusted to 10 on the fluorescence scale. This means that nuclear condensation was not taken into account.

The DNA leakage from the DNA masses was assessed using agarose gels. Nuclei were isolated according to standard method in the isolation buffer, and the DNA leakage was measured by taking a sample from the buffer. The same was done after standing of the isolation buffer with the nuclei for 1 h at 28°C. As DNA will be present at low concentration only, it was concentrated using the macromolecular carrier and isopropanol precipitation. Sodium acetate solution (3 M) and a macromolecular carrier for DNA (Ethachinmate, Nippon gene, Toyama, Japan), were added to the isolation buffer and mixed. This was done just after using the standard procedure for the isolation buffer. The isolation buffer was then immediately mixed with an equal volume of isopropanol and centrifuged for 30 min at 22,400*g*. The precipitate was washed with 70% ethanol and dissolved in 10 mM Tris–HCl (pH 8) containing 10 mM EDTA. The precipitate solution was electrophoresed in a 3% agarose gel and stained with SYBR Gold.

## Total number of DNA masses per corolla

The number of DNA masses was measured by extraction of the nuclei as described and flow cytometry as described. The DNA masses were extracted from a whole corolla using 1.5 ml of buffer. The final volume of the extraction was adjusted to 2 ml, using the buffer solution. A quarter aliquot of the total extraction volume (0.5 ml) was used to measure the number of DNA masses, using flow cytometry. The data were multiplied by 4 to obtain the number of DNA masses per corolla. This was done at $t$=0, 6, 12, 18, 24, 30, 36, 42, and 48 h, using five replications (flowers).

## Morphological analysis

Nuclei and DNA masses were isolated as described for flow cytometry. Isolated DNA masses were stained with DAPI, which stains DNA, and/or with 3,3′-dihexyloxacarbocyanine iodide ($DiOC_6$), which stains lipophilic materials. The DNA masses were observed under a fluorescence microscope (model PROVIS AX70, Olympus, Tokyo, Japan) using U excitation (330–385 nm) for DAPI and IB excitation (460–490 nm) for $DiOC_6$. Digital pictures of DNA masses were obtained for each stain using a low light cool CCD camera (model DP30BW, Olympus). Images of DNA masses stained with DAPI and $DiOC_6$ were overlaid by Meta Morph Version 6.2r6 software (Universal Imaging Corp., Downingtown, PA, USA). The diameter of the DNA masses on the pictures was measured by SimpleDigitizer version 3.01. The average diameter was calculated from 100 DNA masses, randomly selected from pictures.

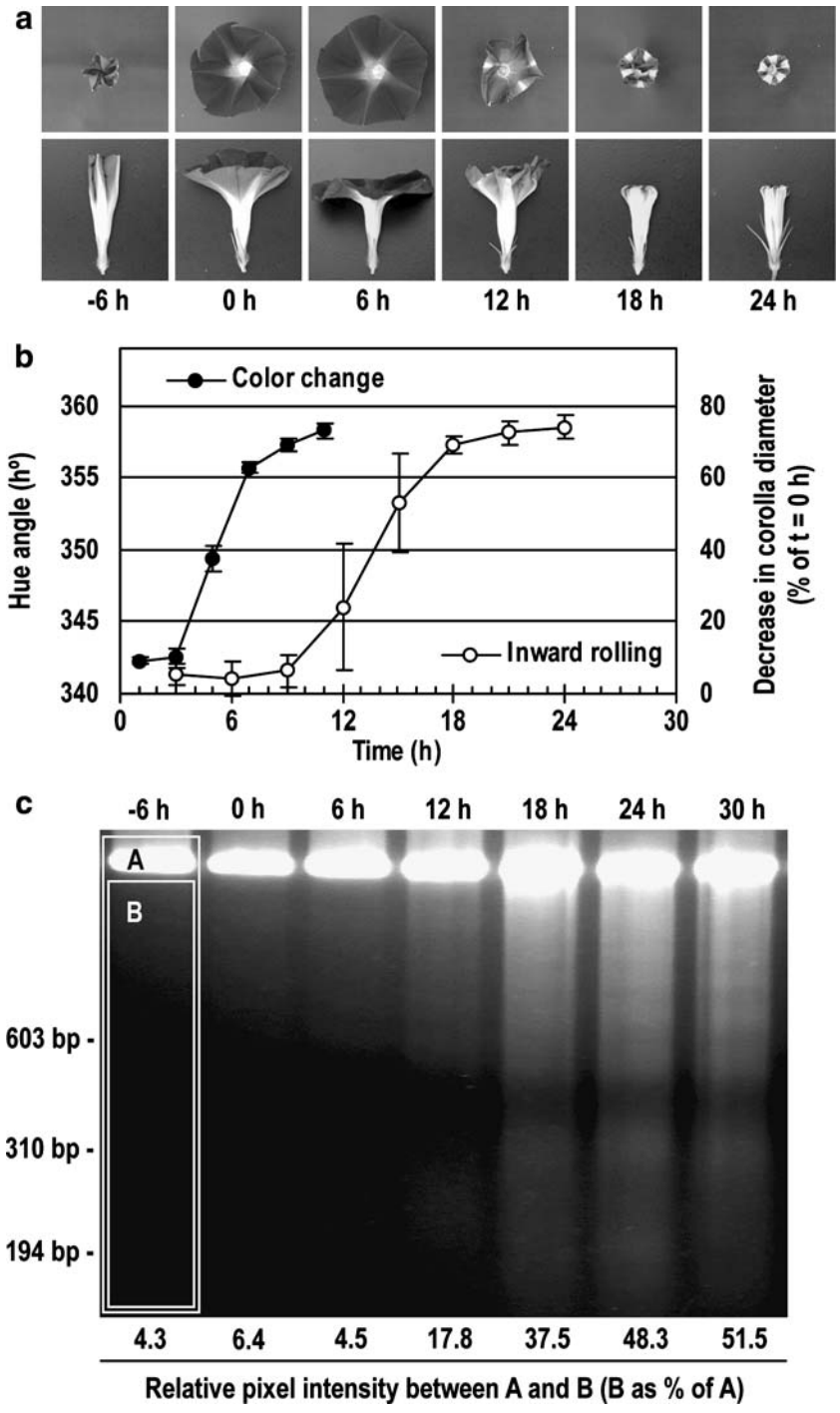


**Fig. 1** Time course of visible senescence and DNA degradation in the petals of *Ipomoea nil*. **a** Stages of flower life. **b** Visible petal senescence. Colour change was assessed by the detection of hue angle of the petals, using a colorimetric method. Inward rolling was calculated as a percentage of decrease in diameter from the maximum diameter of the corolla. **c** DNA degradation. The degradation index, shown under each lane, is the signal intensity of fragmented DNA as a percentage of total DNA on the gel. In **b**, values are means ± SD of at least three separate experiments using five flowers each. In **c**, values are means of three flowers

Treatment with chemicals; ethylene production

Flowers were excised at $t$=0 h and then transferred to sterile distilled water as a control or aqueous solutions of either 1 mM CHI or 1 mM aminoethoxyvinyl glycine (AVG). Cut flowers were put into closed 70 l clear plastic chambers containing fresh air (control) or 1 μl $l^{-1}$ ethylene, with or without 2 μl $l^{-1}$ 1-methylcyclopropene (1-MCP), at 24±1°C under continuous illumination (100 μmol $m^{-2}$ $s^{-1}$).

Ethylene production was measured after careful excision of the petal from flowers treated with AVG or CHI, and then enclosed in a 50-ml glass vial flushed with ethylene-free air. After 1 h of incubation under the same conditions as the cut flowers, ethylene in the 2 ml of headspace gases was detected using a gas chro-

matograph (model GC−14B, Shimadzu, Kyoto, Japan) equipped with a flame ionisation detector (model C-R6A, Shimadzu) and a 100-cm stainless steel column packed with activated alumina. The column temperature was 80°C and the detector was 100°C, with a nitrogen gas pressure of 40 kPa.

### Statistics and repeat experiments

All experiments used at least five replications (flowers), and were repeated at least once at a later date. When indicated the data of several repeat experiments were averaged. The data of Figs. 2a and 6 were analysed by multiple comparison using Fisher's Protected Least Significant Difference (PLSD) method at 1% level.

## Results

### Time line of visible senescence symptoms; DNA degradation

We designated the onset of the light period (0800 hours), as time 0 ($t$=0 h). The flowers were then almost fully open (Fig. 1a). The flower started to open at about 0500 hours ($t$=−3 h) and, depending on the flower, was fully open between 1100 and 1300 hours ($t$=3–5 h; results not shown). The first visible symptom of senescence was a colour change from blue-red to red-purple, which started at about 1100 hours and was complete by 1900 hours ($t$=11 h; Fig. 1b). The onset of the colour change was followed by inward rolling of the petals, starting at about $t$=9 h and complete by $t$=24 h. Inward rolling was due to turgor loss of the cells, which started at the distal petal edge, both in the midribs and in the tissue between the ribs. Rib movement was apparently the main force behind inward rolling.

The DNA degradation was observed using agarose gel analysis (Fig. 1c). The gels of material extracted at $t$=−6 to 6 h showed a little degradation. A considerable increase in degradation was observed from $t$=12 to 30 h. Faint DNA laddering was observed at $t$=24 and 30 h.

### Increase in the number of DNA masses

We tested the idea that the DNA masses can fragment, either inside the nuclear envelope or as a result of nuclear fragmentation. The whole corolla was excised at intervals and total number of DNA masses per corolla was counted. This number increased from about 120,000 at $t$=0 h to about 260,000 at $t$=18 h, and then decreased (Fig. 2a). As described in the following section, the method fails to detect masses with very small DNA fluorescence. This is shown by the cut-off values at the right side of each panel in Fig. 2b.

Part of the increase in DNA masses might be due to mitosis. In the first six panels in Fig. 2b, the small peak at the right represents mitotic nuclei (called G2/M). At $t$=0 h the area under the small peak indicated that the number of mitotic nuclei was 6.4% of the total number of nuclei. At later stages this percentage was similar or smaller, until $t$=24 h when no more mitosis was found.

### Flow cytometric determination of DNA fluorescence

The results of the flow cytometric method are shown in Fig. 2b. In these tests the method determined fluorescence per DNA mass in 10,000 masses. In the first five panels the large peak above the 10 mark represents nuclei that are not mitotic, and not in the process of DNA degradation (called G0/G1). The part to the left of the high peak represents DNA masses with a lower fluorescence than that of the masses in the large peak. The percentage of DNA masses with such decreased DNA level is shown above the bars. This percentage showed a small increase from $t$=−6 to 12 h. It increased sharply from $t$=12 h with a rate that was sustained until $t$=48 h.

We tested the assumption that the detergent in the extraction medium and in the staining medium permeabilises the nuclear envelope which would lead to leakage of DNA fragments to the medium. The staining medium is different from the extraction medium, at least because it does not have a detergent and it contains the fluorescent stain (DAPI). We visualised DNA fragments on agarose gels. However, stained DNA could not be used to run on gels. Therefore only the extraction medium was used, using petals sampled at $t$=0 and 24 h. The medium was sampled just after isolation of the nuclei and after 1 h after incubation in extraction medium at 20°C. The agarose gels showed absence of DNA fragment leakage into the medium (Fig. 2c). The absence of leakage indicated that the decrease in DNA fluorescence during PCD was due to biological factors rather than to a methodical error.

The data on DNA degradation (pixel count on agarose gels), the number of DNA masses, and fluorescence of 10,000 DNA masses are put together in Fig. 3. DNA degradation as here expressed started 6 h later than the increase in DNA masses. DNA degradation then occurred parallel to the increase in DNA masses up to $t$=18 h, when the number of masses decreased but DNA degradation continued. The decrease of fluorescence also paralleled the DNA degradation data, although it started at about 6 h after the onset of DNA degradation.

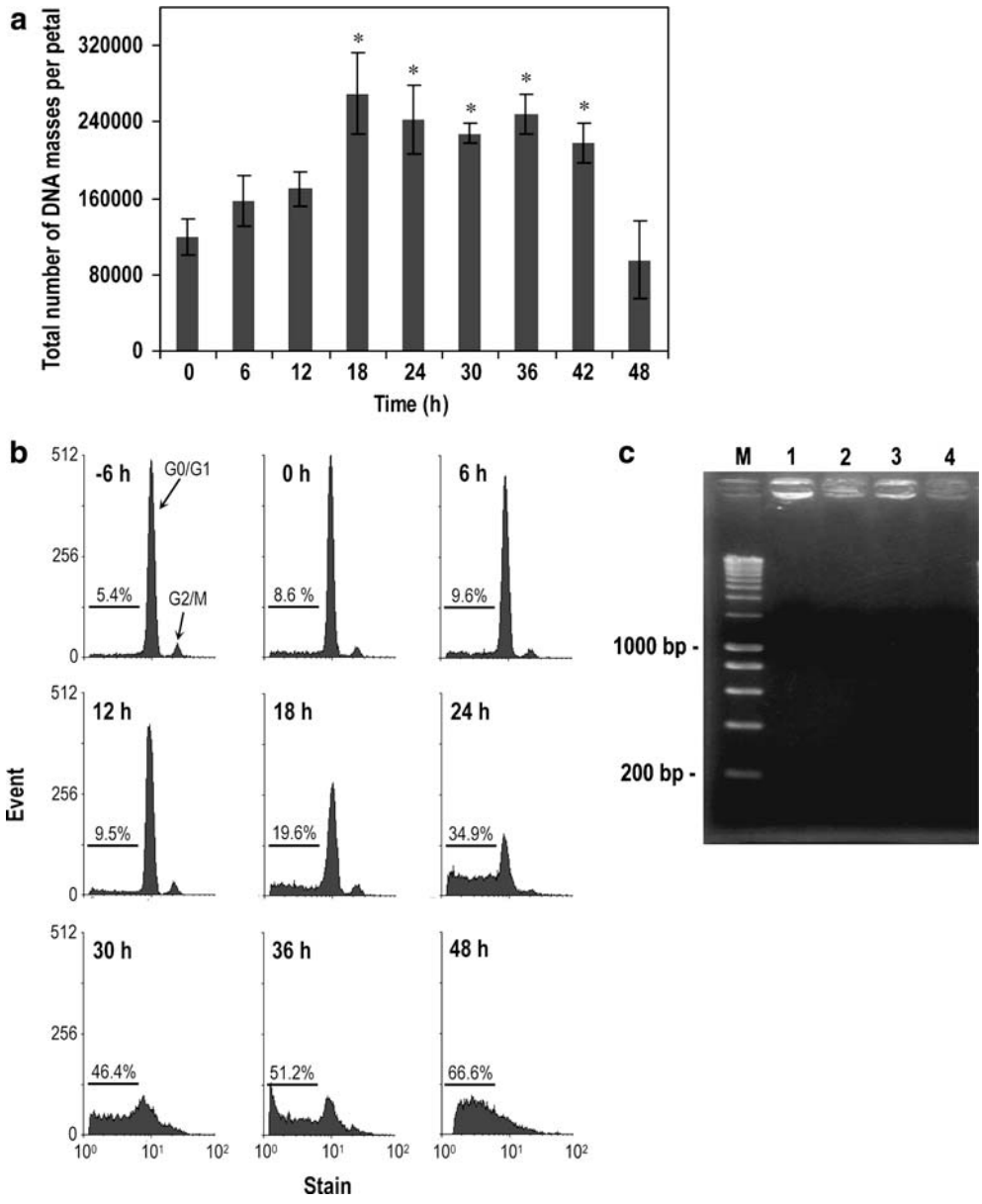


**Fig. 2** Number and fluorescence of DNA masses in the petals of *Ipomoea nil*, during senescence. **a** Total number of DNA masses in the corolla (all petals), determined using flow cytometry. Values are means ± SD of five separate experiments. The *asterisks* show significant differences at the 1% level, compared to *t*=0 h (LSD=96,899). **b** Fluorescence of DAPI-stained DNA masses. Histograms were obtained by flow cytometry of about 10,000 masses. The *arrows* in the first panel indicate the peaks believed to correspond to nuclei during a normal cell cycle. The percentage of DNA masses with fluorescence less than those in the G0/G1 peak is shown *above the bars* (left of the G0/G1 peak). Values are means of at least three separate experiments using five flowers each. Note that the cut-off point (fluorescence is below the detection limit) in these measurements was placed slightly offset to the right with respect to $10^0$. **c** Assessment of DNA fragments leakage from nuclei into the extraction medium during preparation and flow cytometry measurement. At *t*=0 and 24 h DNA in the medium was concentrated, then electrophoresed in a 3% agarose gel and stained with SYBR Gold nucleic acid gel stain. This DNA concentration step was made 1 h after incubation in the medium (*lanes 1 and 2*) or just after the isolation of the nuclei (*lanes 3 and 4*). *Lanes 1 and 3* refer to *t*=0 h, and *lanes 2 and 4* to *t*=24 h. *M* DNA ladder marker

## Chromatin condensation, diameter of DNA masses, presence of nuclear membranes

Fluorescence microscopy of DAPI-stained nuclei from *t*=0 h showed a chromatin distribution typical for normal interphase cells. The chromatin in these nuclei was slightly unevenly distributed as both brighter spots and darker ones were observed (Fig. 4a). At *t*=0 h few nuclei showed condensed chromatin and a smaller nuclear diameter (results not shown). At *t*=12 h numer-

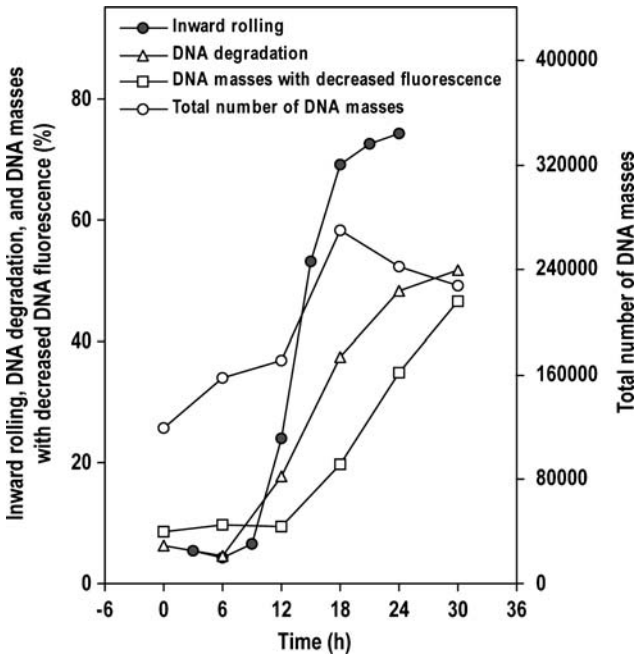


**Fig. 3** Comparison of the data on petal inrolling, DNA degradation as observed on agarose gels, number and fluorescence of DNA masses in *I. nil* petals, during programmed cell death. Index of inrolling is the percentage of maximum diameter, from Fig. 1b. DNA degradation is shown as relative pixel intensity from Fig. 1c. The total number of DNA masses is derived from Fig. 2a. The data on the fluorescence per DNA mass are taken from Fig. 2b

ous nuclei showed chromatin condensation, as they showed brighter DNA fluorescence than normal nuclei. The diameter of these nuclei with condensed chromatin was about 70% of that of normal ones. Chromatin fluorescence in the nuclei with condensed chromatin was unevenly distributed, with brighter spots throughout the nucleus (Fig. 4b). At *t*=24 h many DNA masses were quite small. Most of the DNA masses then still had bright DNA fluorescence. The smallest observed DNA masses had a diameter less than 10% of that of the original nucleus (Fig. 4c).

Measurement of the diameter of the nuclei at *t*=0 h revealed a rather wide Gaussian-like distribution. Diameters varied from about 8 to 18 μm, with an average of about 13 μm (Fig. 5). At *t*=12 h there were two apparent Gaussian-like distribution curves, one similar to the one at *t*=0 h, and one containing smaller nuclei. At *t*=24 h the group of *t*=0 h had almost disappeared, while the group of smaller DNA masses assumed a more clearly Gaussian-like curve. At this time (*t*=24 h) the average diameter of the DNA masses was about half of that at *t*=0 h. At later sampling times, the distribution curve gradually shifted to smaller average diameters (Fig. 5).

Light microscopy of unstained nuclei and fluorescence microscopy of DAPI- stained nuclei and DNA masses indicated the presence of a membrane around each mass, at least at *t*=0, 12 and 24 h (results not shown). Staining with the cationic lipophilic fluorochrome $DiOC_6$ indicated the presence of a membrane at *t*=48 h (Fig. 4d–i). Figure 4c shows that DNA masses with a diameter of about one-fifth of the original were stained with $DiOC_6$. The DNA masses with a smaller diameter also showed $DiOC_6$ staining.

In contrast, the DNA masses that were treated with $DiOC_6$ at earlier stages of development than a nuclear diameter of about one-fifth of original did not stain with $DiOC_6$.

### Effects of cycloheximide, ethylene, and ethylene inhibitors

When flowers were continuously treated with cycloheximide (CHI), starting at *t*=0 h, petal inrolling was prevented (Fig. 6a). In contrast, continuous treatment with 1-MCP, also starting at *t*=0 h, did not suppress inrolling (Fig. 6a). Exposure to ethylene accelerated inward rolling (Fig. 6b). When flowers were treated with both ethylene and CHI, inrolling was arrested to the same extent as flowers that were treated with CHI alone (Fig. 6b). 1-MCP suppressed petal inward rolling to the level of controls that were left untreated (Fig. 6b).

No decrease in DNA per DNA mass occurred if the flowers were treated with CHI (Fig. 6c). In contrast, treatment with AVG or 1-MCP did not affect the DNA per DNA mass (Fig. 6c), but ethylene treatment advanced it (Fig. 6d). This ethylene effect was counteracted by 1-MCP. Treatment with CHI prevented DNA degradation even in petal treated with ethylene (Fig. 6d).

### Ethylene production

In control flowers, ethylene production by the petals increased sharply and reached a maximum at *t*=3 h (Fig. 7). If flowers were treated with CHI, starting at *t*=0 h, ethylene production of the petals was still the same 1 h after the onset of treatment but was much less than in controls from *t*=2 h. It reached a minimum at *t*=4 h (Fig. 7). AVG treatment, starting at *t*=0 h, had a much more drastic effect. It suppressed ethylene production to very low levels within 1 h of application (Fig. 7).

## Discussion

Our main findings are: (1) a large increase in the number of DNA masses per petal, (2) a drastic decrease in the average diameter of these masses, and (3) the pres-

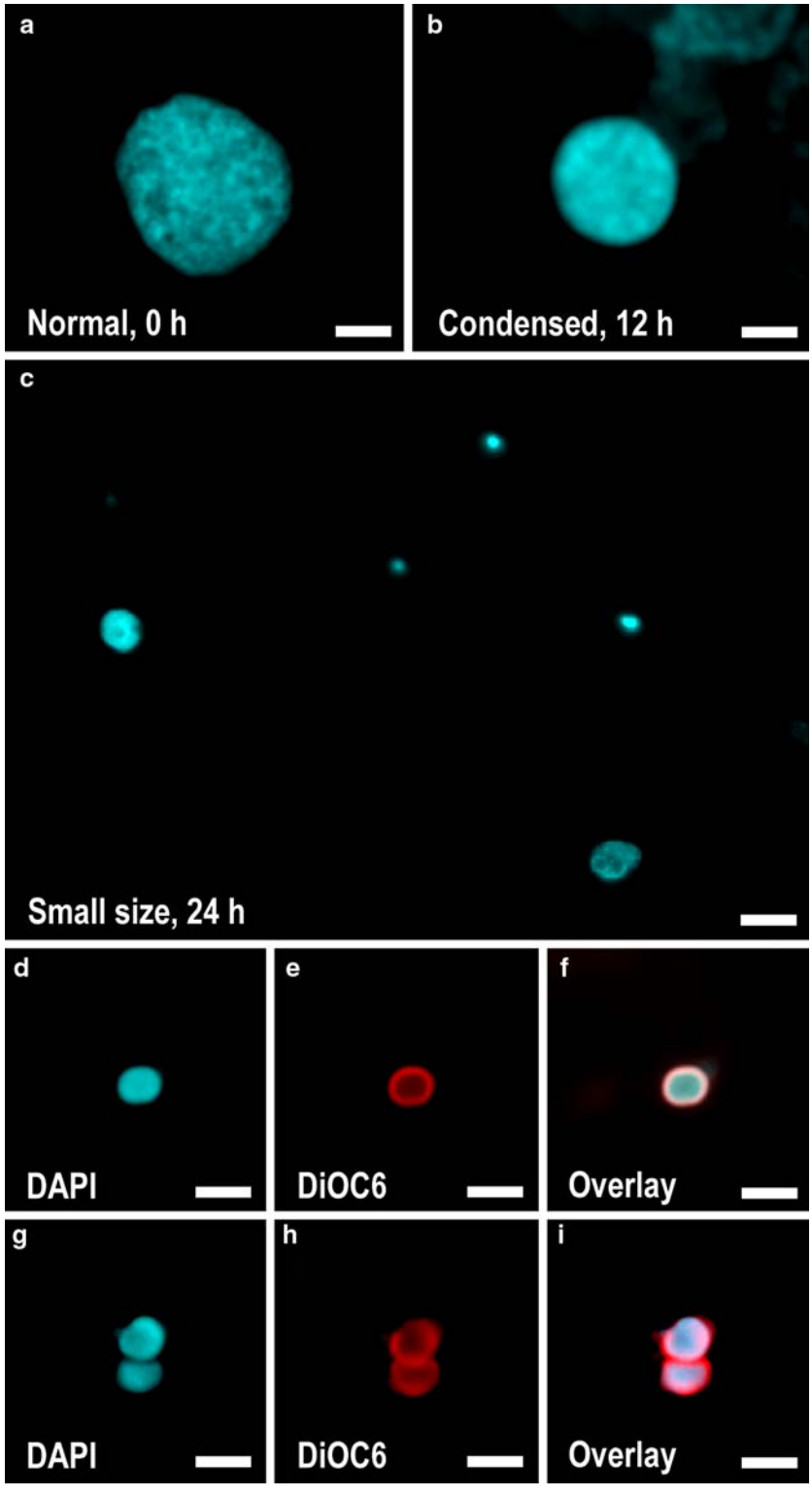


**Fig. 4** **a–i** Nuclear morphology during programmed cell death in *Ipomoea nil* petals. **a–c** Comparison of the shapes and fluorescence. The micrographs show typical examples of **a** normal mesh-like structure of chromatin at *t*=0 h, **b** chromatin condensation observed at *t*=12 h, and **c** small nuclei observed at *t*=24 h. **d–i** Staining of DNA and the nuclear membrane. Nuclei, isolated at *t*=48 h, were stained with DAPI, a fluorochrome for DNA and/or with $DiOC_6$, for the nuclear membrane. Nuclei were observed using a fluorescence microscope under (**d**, **g**) U or (**e**, **h**) IB excitations. All bars = 5 μm

ence of membranes surrounding even small DNA masses. The hypotheses in the present experiments were: (a) nuclear DNA degradation in *Ipomoea* petal cells occurs prior to cellular collapse, and (b) nuclear fragmentation occurs in these cells. The results do not contradict the hypotheses.

The presently found DNA degradation prior to cellular collapse is similar to that reported, for example, in *Iris* petals (van der Kop et al. 2003; van Doorn et al. 2003) and is different from the data on PCD in *Zinnia* leaf mesophyll cells which are induced to differentiate into tracheary elements. In these cells the nucleus and

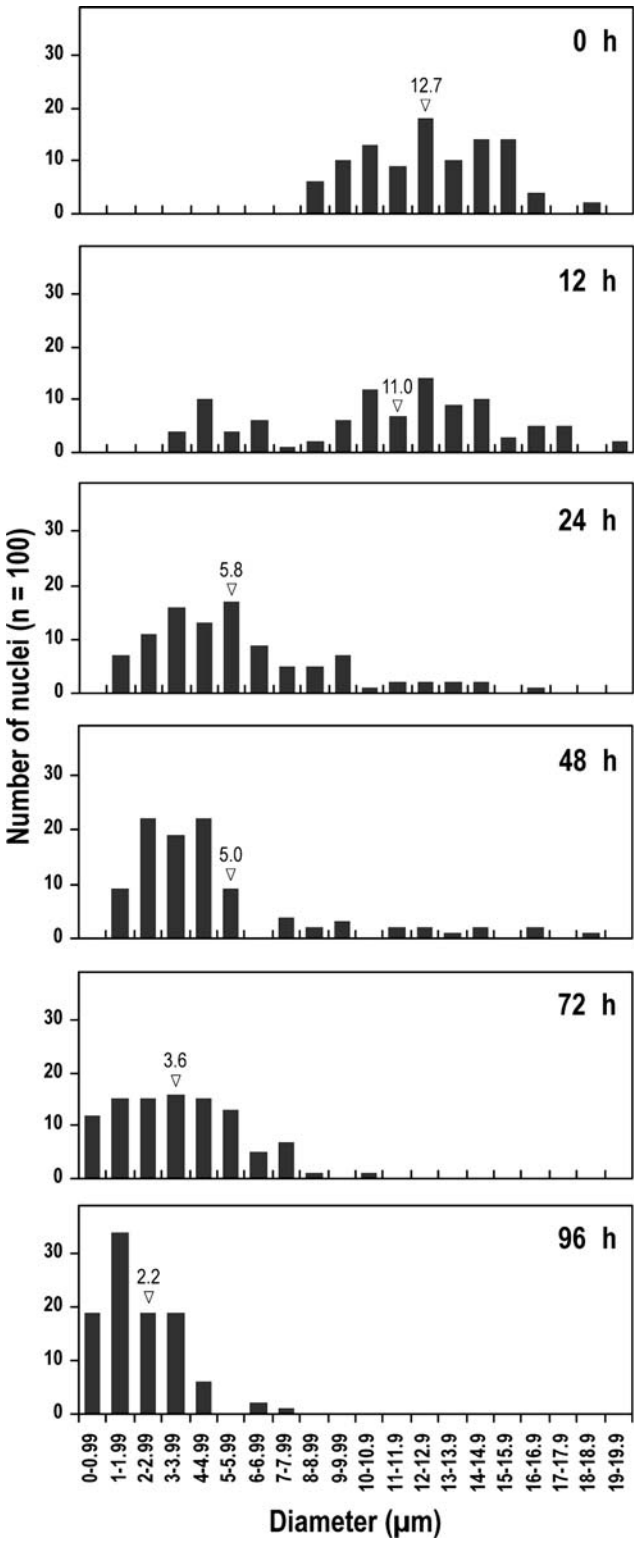


**Fig. 5** Diameters of nuclei isolated from *I. nil* petals, during programmed cell death. Histograms were obtained by measurement of 100 DNA masses. The *arrowhead and numeric value* indicate average diameter

its contents became degraded only after collapse of the vacuole (Obara et al. 2001).

Using flow cytometry, we detected that the number of DNA masses nearly doubled. Figure 2b shows a small peak of mitotic nuclei, to the right of the main peak, until $t$=24 h. The small size of the peak indicates a low number of dividing cells. At $t$=0 h the area under the small peak represented 6.4% of the total number of nuclei. This indicates that the number of new nuclei produced by mitosis cannot account for the doubling of the DNA masses. Microscopy did not show where the mitotic nuclei were located. A large part of the increase in the number of DNA masses, therefore, is apparently accounted for by chromatin fragmentation or nuclear fragmentation.

The flow cytometry method used has a fluorescence detection limit. As can be seen from Fig. 2b, there is a sharp cut-off of the DNA masses at this detection limit, already at $t$=18–24 h. This indicates that a considerable number of nuclei remained undetected. The decrease in the total number of nuclei, after $t$=18 h, therefore, might be an experimental artefact. From $t$=18 h the total number of nuclei might stay the same or even increase.

The data indicate that increase in the number of DNA masses was apparently mainly due to nuclear fragmentation, not to chromatin fragmentation within the same nuclear envelope. At least until $t$=24 h, the DNA masses (some of these were nuclei) apparently had an envelope. Only by $t$=48 h a structure surrounding the DNA masses stained with $DiOC_6$, a cationic fluorochrome that stains all intracellular membranes (Tarin and Cano 1998). We infer that the fluorochrome stained a membrane surrounding the DNA masses. We also surmise that, although the surrounding membrane was not shown by $DiOC_6$ staining prior to $t$=48 h, it was present. Prior to $t$=48 h the membrane composition apparently did not allow staining by the cationic $DiOC_6$. Matzke et al. (1988) showed that $DiOC_6$ sometimes does not stain the nuclear membrane. The presence of certain membrane proteins or a large transmembrane potential seemed to prevent binding of this fluorochrome. The removal of such proteins from the membrane or the disappearance of most of the membrane potential might explain why $DiOC_6$ staining in our experiments only occurred late. Our data thus indicate nuclear fragmentation into DNA masses each surrounded by a membrane. This seems similar to a report on PCD in roots. Schussler and Longstreth (2000) showed EM photographs of PCD in *Sagittaria alismatifolia* roots, indicating that the nucleus was breaking apart into fragments that were each surrounded by a double membrane. However, the fragments were not shown to become completely separated.

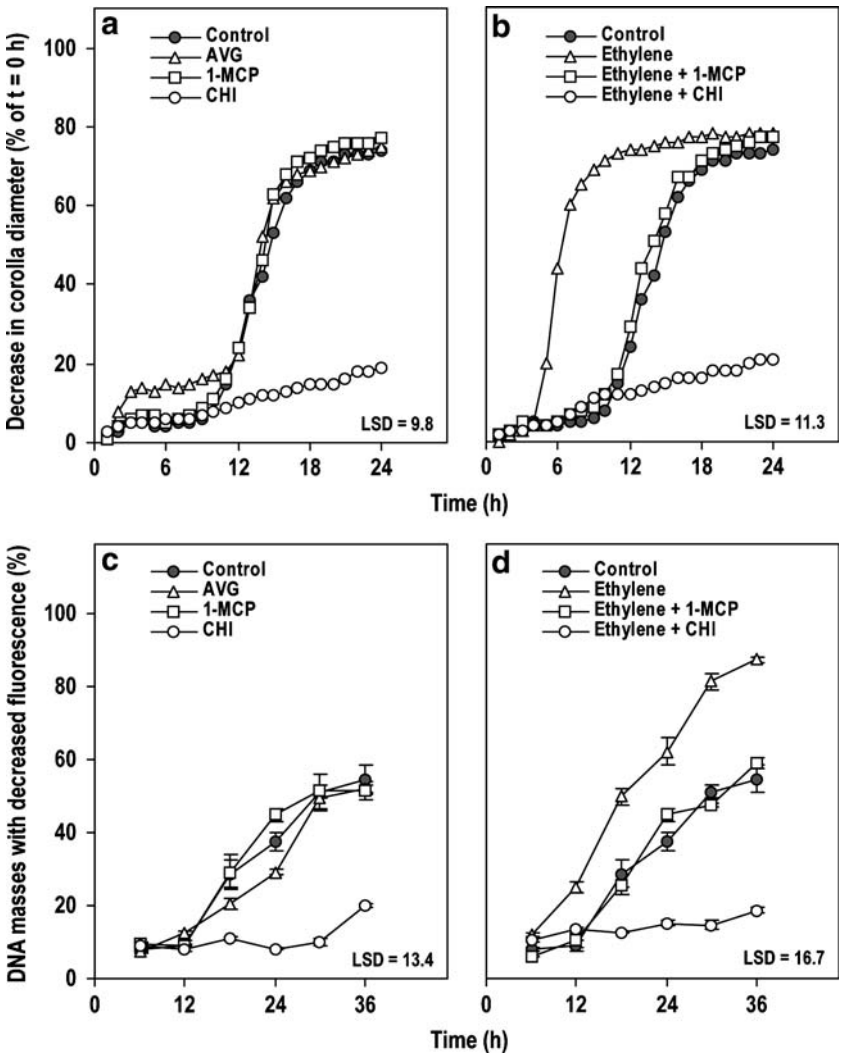


**Fig. 6** Effects of a protein synthesis inhibitor (cycloheximide, CHI), ethylene inhibitors (AVG and 1-MCP), and ethylene on visible senescence and the fluorescence of DNA masses in the petals of *I. nil*, during programmed cell death. Petal inrolling after treatment with (**a**) inhibitors and (**b**) inhibitors together with ethylene. Fluorescence of nuclei of flowers treated with (**c**) inhibitors and (**d**) inhibitors together with ethylene. In **a**, **b**, values are means of three separate experiments using five flowers each. In **c**, **d**, values are means ± SD of two separate experiments using three flowers each. Multiple comparisons were performed using Fisher's PLSD method at 1% significance level. LSD values were included in each frame

Chromatin condensation was observed from $t$=0 h. The condensation followed from an increase in fluorescence per unit surface, and from a decrease in nuclear size. At later stages of PCD, most DNA masses, including quite small ones, still exhibited bright fluorescence, which indicated that the chromatin was still condensed.

At $t$=12 h many nuclei with condensed chromatin were found. At this time also two populations of nuclei were observed, one with a diameter that was about half of the original. The group with the relatively small diameter might consist of several types of nuclei. One subpopulation might be a group of condensed nuclei, with a diameter somewhat bigger than half of original, and the other groups might include nuclei that have (1) fragmented or (2) in which much DNA has been degraded, or (3) nuclei in which both fragmentation and considerable DNA degradation has taken place. It is at this point not possible to distinguish between these categories. At later stages of PCD the DNA masses became increasingly smaller. Again, our data do not allow to distinguish between (further) fragmentation and and/or a decrease in mass as a result of DNA degradation.

The following order was observed between the senescence parameters studied: (1) chromatin condensation, at least from $t$=0 h, (2) an increase in the number of DNA masses, at least from $t$=0 h (Fig. 3), (3) a petal colour change from blue-red to more purple red, from $t$=3 h (Fig. 1), (4) DNA degradation and petal inrolling, from $t$=6 h (Fig. 3), and (5) from $t$=12 h a detectable decrease in average fluorescence of the DNA masses (Fig. 3) and at least by that time a decrease in average diameter of the DNA masses (Fig. 5).

The observed change in colour has also been reported in *Ipomoea tricolor* (Winkenbach 1970). Petal colour changes during senescence have been attributed to change in vacuolar pH which affected anthocyanins (Asen et al. 1971), (4) from $t$=6 h a decrease of flower diameter (inward rolling of the petal) associated with

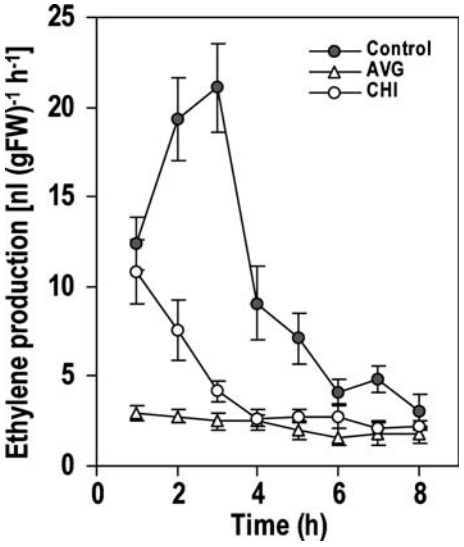


**Fig. 7** Ethylene production in *I. nil* flowers treated with a protein synthesis inhibitor or ethylene inhibitors. Flowers were excised at *t*=0 h and transferred to sterile distilled water (control) or aqueous solution of the protein synthesis inhibitor cycloheximide (CHI) or the ethylene synthesis inhibitor AVG. Ethylene production was measured using gas chromatography. Values are means ± SD of at least two separate experiments using four flowers each

PCD-related turgor loss, i.e. cellular death. Previous reports showed that the PCD in *Ipomoea* petals started at distal margin where the upper epidermal cells lost turgor and died earlier than those at the lower epidermis. This explains the inward rolling. Cell death then proceeded towards the petal base (Winkenbach 1970; Hanson and Kende 1975).

We confirmed the previous finding that cycloheximide prevents inward rolling in *Ipomoea* (Baumgartner et al. 1975), and found that it also blocked the decrease of DNA fluorescence per DNA mass. This suggested a common control point, involving protein synthesis, of the two parameters. We also confirmed that ethylene hastens inward rolling (Kende and Baumgartner 1974), but contrary to the conclusion of these authors, we found no evidence for a role of endogenous ethylene in the regulation of inward rolling. Kende and Baumgartner (1974) based their conclusion on the inhibiting effect of carbon dioxide on inward rolling. Carbon dioxide, however, is not a specific ethylene antagonist. With AVG or 1-MCP, potent and specific ethylene antagonists, we now found no effect on flowers that were not treated with ethylene, whereas in the ethylene-treated flowers these antagonists only abolished the ethylene effect. This means that the normal process is not regulated by endogenous ethylene. Increased ethylene production, by stress or pollination, thus at most hastens natural PCD, whereas normal PCD is not regulated by endogenous ethylene. This is reminiscent of the role of ethylene in leaf yellowing in *Arabidopsis*, where it was also found to hasten the onset of yellowing, whereas it was neither involved in the rate of yellowing nor in the timing of the normal onset of yellowing (Grbic and Bleecker 1995).

It is concluded that the PCD in *Ipomoea* petal was accompanied by a remarkable increase in the number of DNA masses. This increase was apparently due to nuclear fragmentation, because the DNA masses seemed surrounded by a membrane each. A large ongoing decrease of the diameter per DNA mass was observed, with masses the diameter of which was less than 10% of original. The data indicate lack of control by endogenous ethylene of petal inward rolling and the changes in nuclear parameters studied. The time to petal inward rolling symptom in this species, therefore, is not due to endogenous ethylene, even though it could be hastened by exogenous ethylene.

## References

Asen S, Norris KH, Stewart RN (1971) Effect of pH and concentration of the anthocyanin–flavonol co-pigment on the color of 'Better Times' roses. J Am Soc Hortic Sci 96:770–773

Baumgartner B, Hurter J, Matile P (1975) On the fading of an ephemeral flower. Biochem Physiol Pflanz 168:299–306

Beutelmann P, Kende H (1977) Membrane lipids in senescing flower tissue of *Ipomoea tricolor*. Plant Physiol 59:888–893

Boe R, Gjertsen BT, Vintemyr OK, Houge G, Lanotte M, Doskeland SO (1991) The protein phosphatase inhibitor okadaic acid induces morphological changes typical of apoptosis in mammalian cells. Exp Cell Res 195:237–246

Danon A, Gallois P (1998) UV-C radiation induces apoptotic-like changes in *Arabidopsis thaliana*. FEBS Lett 437:131–136

Dini L, Coppola S, Ruzittu MT, Ghibelli L (1996) Multiple pathways for apoptotic nuclear fragmentation. Exp Cell Res 223:340–347

van Doorn WG, Woltering EJ (2005) Many ways to exit? Cell death categories in plants. Trends Plant Sci 10:117–122

van Doorn WG, Balk PA, van Houwelingen AM, Hoeberichts FA, Hall RD, Vorst O, van der Schoot C, van Wordragen MF (2003) Gene expression during anthesis and senescence in *Iris* flowers. Plant Mol Biol 53:845–863

Grbic V, Bleecker AB (1995) Ethylene regulates the timing of leaf senescence in *Arabidopsis*. Plant J 8:595–602

Hanson AD, Kende H (1975) Ethylene-enhanced ion and sucrose efflux in morning glory flower tissue. Plant Physiol 55:663–669

Hockenbery D (1995) Defining apoptosis. Am J Pathol 146:15–19

Kende H, Baumgartner B (1974) Regulation of aging in flowers of *Ipomoea tricolor* by ethylene. Planta 116:279–289

van der Kop DAM, Ruys G, Dees D, van der Schoot C, de Boer AD, van Doorn WG (2003) Expression of *defender against apoptotic death (DAD-1)* in *Iris* and *Dianthus* petals. Physiol Plant 117:256–263

Marubashi W, Yamada T, Niwa M (1999) Apoptosis detected in hybrids between *Nicotiana glutinosa* and *N. repanda* expressing lethality. Planta 210:168–171

Matile P, Winkenbach F (1971) Function of lysosomes and lysosomal enzymes in the senescing corolla of the morning glory (*Ipomoea purpurea*). J Exp Bot 22:759–771

Matzke MA, Matzke AJM, Neuhaus G (1988) Cell age-related differences in the interaction of a potential-sensitive fluorescent dye with nuclear envelopes of *Acetabularia mediterranea*. Plant Cell Environ 11:157–164

McGuire RG (1992) Reporting of objective color measurements. Hortic Sci 27:1254–1255

Obara K, Kuriyama H, Fukuda H (2001) Direct evidence of active and rapid nuclear degradation triggered by vacuole rupture during programmed cell death in zinnia. Plant Physiol 125:615–626

Schussler EE, Longstreth DJ (2000) Changes in cell structure during the formation of root aerenchyma in *Sagittaria lancifolia* (Alismataceae). Am J Bot 87:12–19

Sun Y, Clinkenbeard KD, Ownby CL, Cudd L, Clarke CR, Highlander SK (2000) Ultrastructural characterization of apoptosis in bovine lymphocytes exposed to *Pasteurella haemolytica* leukotoxin. Am J Vet Res 61:51–56

Tarin JJ, Cano A (1998) Distribution of 5-chloromethylfluorescein diacetate staining during meiotic maturation and fertilization in vitro of mouse oocytes. J Reprod Fertil 114:211–218

Wang H, Li J, Bostock RM, Gilchrist DG (1996) Apoptosis: a functional paradigm for programmed plant cell death induced by a host-selective phytotoxin and invoked during development. Plant Cell 8:375–391

Winkenbach F (1970) Zum Stoffwechsel der aufblühenden und welkenden Korolle der Prunkwinde *Ipomoea purpurea*. Berichte der schweizischen botanischen Gesellschaft 80:374–390

Yamada T, Marubashi W (2003) Overproduced ethylene causes programmed cell death leading to temperature-sensitive lethality in hybrid seedlings from the cross *Nicotiana suaveolens* × *N. tabacum*. Planta 217:690–698

Yamada T, Takatsu Y, Kasumi M, Manabe T, Hayashi M, Marubashi W, Niwa M (2001) Novel evaluation method of flower senescence in freesia (*Freesia hybrida*) based on apoptosis as an indicator. Plant Biotechnol 18:215–218

Yamada T, Takatsu Y, Manabe T, Kasumi M, Marubashi W (2003) Suppressive effect of trehalose on apoptotic cell death leading to petal senescence in ethylene-insensitive flowers of gladiolus. Plant Sci 164:213–221

Yao N, Eisfelder BJ, Marvin J, Greenberg JT (2004) The mitochondrion—an organelle commonly involved in programmed cell death in *Arabidopsis thaliana*. Plant J 40:596–610